Scaled Experiment to Investigate Auroral Kilometric Radiation Mechanisms in the Presence of Background Electrons

S.L. M^{c}Conville[1], K. Ronald[1], D.C. Speirs[1], K.M. Gillespie[1], A.D.R. Phelps[1], A.W. Cross[1], R. Bingham[1,3], C.W. Robertson[1], C.G.Whyte[1], W. He[1], M. King[1], R. Bryson[1], I. Vorgul[2], R.A. Cairns[2] and B.J. Kellett[3]

[1]SUPA Department of Physics, University of Strathclyde, Glasgow, G4 0NG, Scotland

[2]School of Mathematics and Statistics, University of St. Andrews, St. Andrews, KY16 9SS, Scotland

[3]Space Physics Division, STFC, Rutherford Appleton Laboratory Didcot, OX11 0QX, England

sandra.l.mcconville@strath.ac.uk

Abstract. Auroral Kilometric Radiation (AKR) emissions occur at frequencies ~300kHz polarised in the X-mode with efficiencies ~1-2% [1,2] in the auroral density cavity in the polar regions of the Earth's magnetosphere, a region of low density plasma ~3200km above the Earth's surface, where electrons are accelerated down towards the Earth whilst undergoing magnetic compression. As a result of this magnetic compression the electrons acquire a horseshoe distribution function in velocity space. Previous theoretical studies have predicted that this distribution is capable of driving the cyclotron maser instability. To test this theory a scaled laboratory experiment was constructed to replicate this phenomenon in a controlled environment, [3-5] whilst 2D and 3D simulations are also being conducted to predict the experimental radiation power and mode, [6-9]. The experiment operates in the microwave frequency regime and incorporates a region of increasing magnetic field as found at the Earth's pole using magnet solenoids to encase the cylindrical interaction waveguide through which an initially rectilinear electron beam (12A) was accelerated by a 75keV pulse. Experimental results showed evidence of the formation of the horseshoe distribution function. The radiation was produced in the near cut-off TE_{01} mode, comparable with X-mode characteristics, at 4.42GHz. Peak microwave output power was measured ~35kW and peak efficiency of emission ~2%, [3]. A Penning trap was constructed and inserted into the interaction waveguide to enable generation of a background plasma which would lead to closer comparisons with the magnetospheric conditions. Initial design and measurements are presented showing the principle features of the new geometry.

1. Introduction

Some magnetized planets and stars such as Earth and UV Ceti, exhibit radiation generation at their magnetic poles. For the case of the Earth this radiation emission is known as Auroral Kilometric

Radiation. Approximately 3200km above the Earth's surface there exists a region of plasma depletion known as the Auroral Density Cavity. Particles descend through this region towards the ionosphere following the path of the magnetic field lines. Along their descent the particles undergo magnetic compression. Due to conservation of the magnetic moment there is a transfer of axial to perpendicular velocity leading to a horseshoe shaped distribution function forming in velocity space.

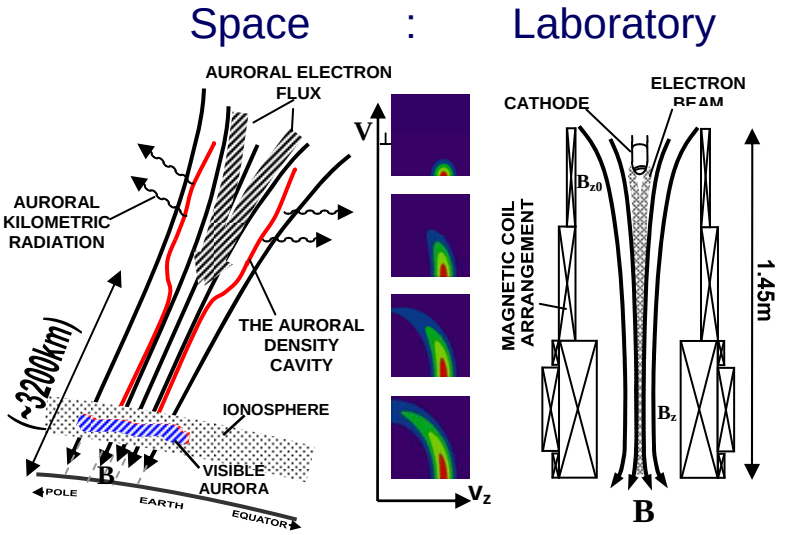

Figure 1: Comparisons in the geometry between magnetospheric and laboratory environment

Figure 1 shows this distribution formation alongside a schematic of the magnetospheric and experimental geometry. The horseshoe distributions have been shown to be unstable to an electron cyclotron resonance maser type of instability [10-12], and are now proposed as the source of free energy responsible for the production of AKR in these regions [13-16]. The emitted radiation has been observed by satellites to be in the X-mode. To provide a controlled environment to study this naturally occurring phenomenon, a scaled laboratory experiment was constructed at Strathclyde University, Figure 1, to replicate the process.

Theoretical studies in this field have been carried out at the University of St Andrews [17,18] where the problem is approached from the kinetic plasma theory point of view. These results correlate well with the experimental and numerical measurements at Strathclyde.

2. Experimental Apparatus

2.1. Magnet Coils

A solenoid system was constructed, Figure 2, which would encompass the electron beam as it traversed through the apparatus, left to right from the cathode region to the anode. The coils are wound individually allowing the magnetic field profile to be varied with a fine degree of precision. Altering the supply current of coil 3 which is the main cavity coil controlled the peak magnetic plateau whilst the ratio of coils 1-3 controls the magnetic compression of the electron beam as it passes through the interaction waveguide where resonance with the waveguide modes will take place. The blue lines in Figure 2 (left to right) show the position of the cathode face and the mid-point of the interaction waveguide respectively.

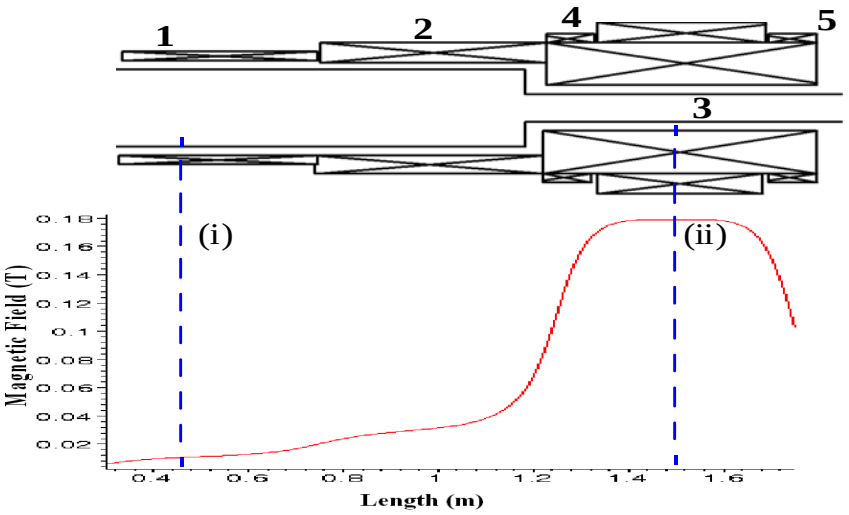

Figure 2: Layout of magnet coils with corresponding magnetic field profile

2.2. Electron Injector

For electron beam generation, an explosive emission cathode was used, Figure 3. As can be seen from the picture there is a velvet ring surrounding the dome of the cathode face. The dome is to provide an initial spread in pitch of the electrons as they leave the cathode, whilst the velvet provides for field emission that occurs at the fibre tips.

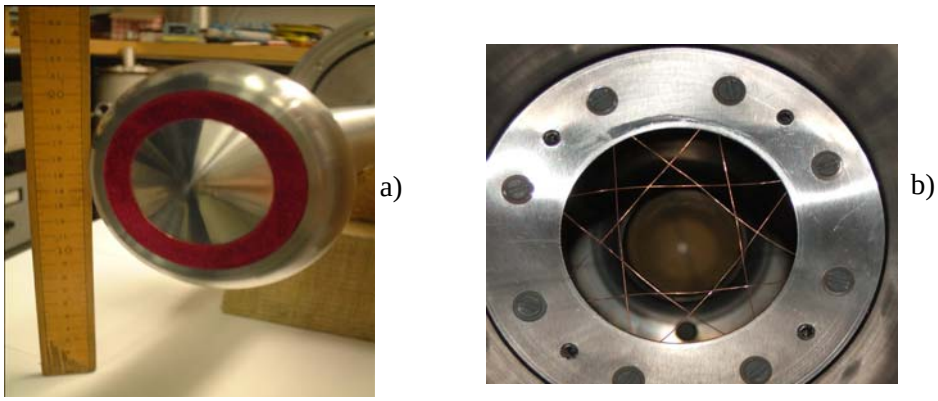

a) b)

Figure 3: a) Cathode face with velvet ring, b) Anode mesh.

The anode mesh which can be seen in Figure 3b) is situated at ~ 2cm away from the cathode face and is designed in a way that will have minimal disruption to the beam as it passes through the copper wires, whilst helping to concentrate the field back at the cathode face thus allowing for lower accelerating voltages to be used during operation.

2.3. Penning Trap

The design for the Penning trap used in the experiment, Figure 4a), was based on the conventional design of two solid cathodes and cylindrical anode creating a trap in which to contain electrons as they collide with gas particles. To allow an electron beam to pass through the trap a 40mm hole was cut in one cathode plate whilst the second cathode plate was replaced with a mesh to allow egress of radiation. The cathode and anode walls of the trap were constructed using copper and were encased in

a nylon jacket to act as an insulator and to prevent the copper walls from touching the walls of the interaction waveguide where it was situated, Figure 4b).

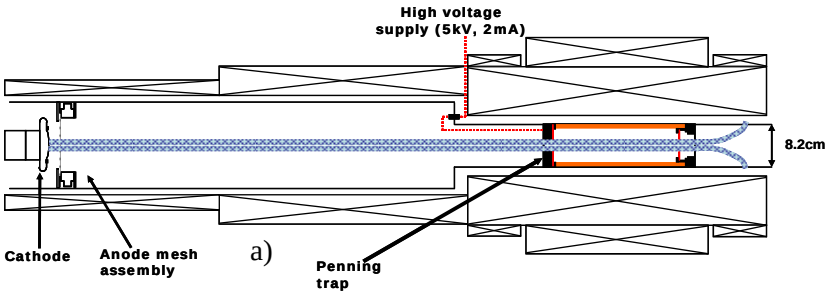

a)

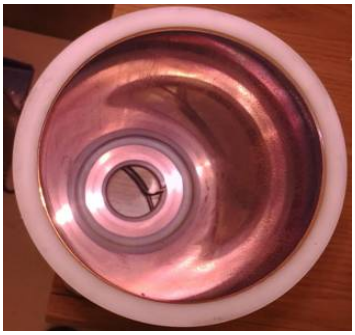

b)

Figure 4: a) Schematic of apparatus showing position of Penning trap inside the interaction region,

b) End view of the Penning trap

A specially designed vacuum feed-through delivered a high voltage (up to +5kV) DC signal to the anode, shown in red in Figure 4a). With the plateau magnetic field set at 0.21T for the TE_{01} resonance in the new dimensions of the interaction region, a voltage was applied to the trap and the anode current and voltage measured. The plateau magnetic field was altered to investigate the effect this had upon the ignition, optical intensity, stability and sustained current and voltage of the discharge.

3. Experimental Results

3.1. Beam Measurements without Penning trap

The initial experiments do not include the Penning trap and so the cyclotron frequency is 4.42GHz, for the interaction waveguide dimension of 4.14cm radius, with an operating plateau magnetic field of 0.18T. With increasing cathode flux density it was seen that the beam current increased as is shown in Figure 5a).

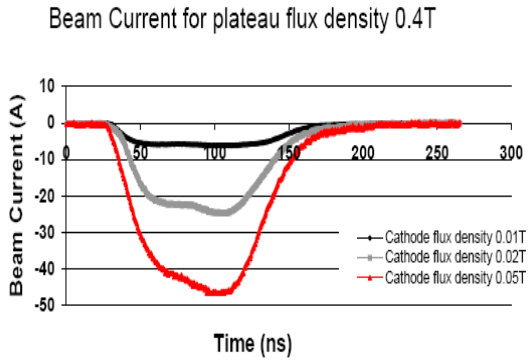

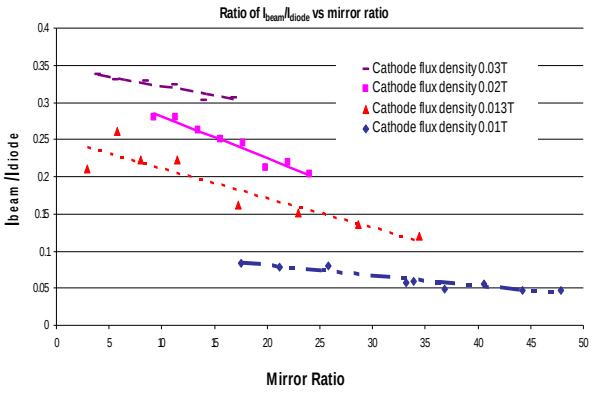

Figure 5: a) Variation of beam current with cathode flux density, b) Effect of increasing plateau magnetic field on beam current measurements

For different cathode flux settings it was seen that with increasing mirror ratio, the measured beam current decreased steadily, showing signs that mirroring was taking place within the experiment and therefore that a horseshoe shape distribution function was forming. This can be seen in Figure 5b).

3.2. Microwave Measurements

Using a fast 12GHz oscilloscope connected to microwave antenna, the operating frequency of the emitted radiation was measured. This was done by capturing the AC waveform signal and performing an FFT on the data giving a value of 4.42GHz, as predicted, and is shown in Figure 6a). The mode scan experiment allowed the mode pattern of the radiation to be plotted and was seen to be that of the TE_{01} mode, as expected, shown in Figure 6b). This mode of operation correlates well with the magnetospheric data where the radiation is polarised in the X-mode. The X-mode shares properties with close to cut-off TE_{01} modes in that they propagate and are polarised perpendicular to the static magnetic field.

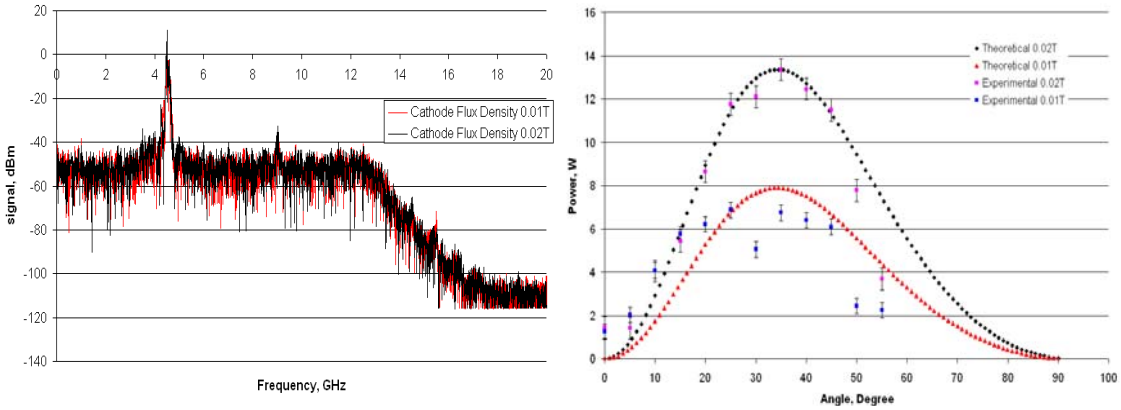

Figure 6: a) Operating frequency of emitted radiation, b) TE_{01} mode pattern obtained through antenna scans

3.3. Penning Trap Characterisation

To establish a stable discharge regime in the Penning trap a range of gasses (Helium, Nitrogen and Argon), pressures ~10^{-6}mBar to 10^{-4}mBar and magnetic field settings were investigated. Figure 7a) shows a graph of the voltage (blue trace) and current (green trace) measured against time. In this particular case the magnetic field is at a setting of 0.27T. Figure 7b) shows an alternative method to plotting the IV characteristics as a straight IV plot with no time axis.

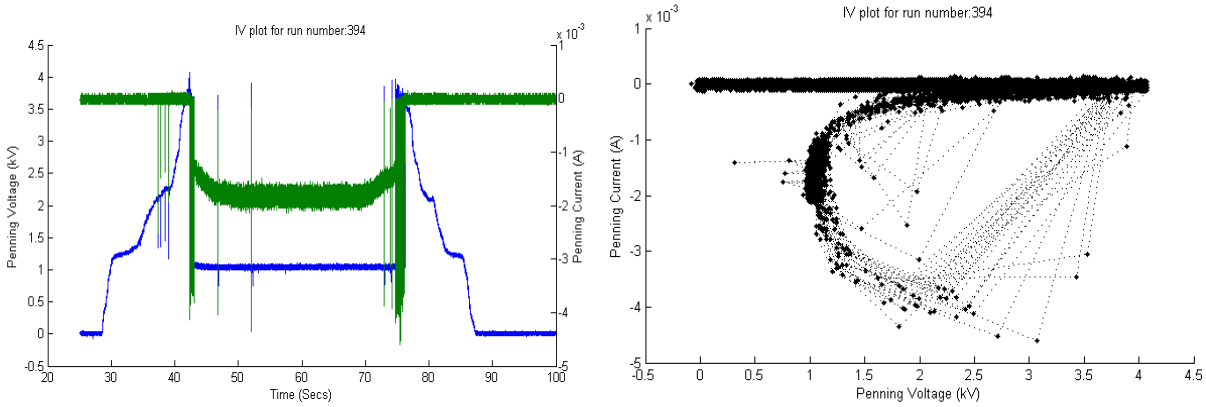

Figure 7: a) IV characteristics of the Penning trap, b) Alternative plot method for IV characteristics

It was found, through an extensive experimental investigation, that the optimum gas and pressure setting for the IV characteristics of the Penning trap was Argon at 10^{-4}mBar, this is plotted in Figure 7a). In general the higher the pressure the less voltage was required to ignite and sustain the discharge.

What can be seen in the above Figure 7 is that as the drive power to the trap was increased, the voltage measured across the trap decreased whilst measured current increased. Both voltage and current attain a steady sustained value once the discharge ignites, before tailing back to zero as the drive power is switched off.

These measurements which characterize the new geometry of the Penning trap will aid in the analysis of results that will be obtained in the future when the Penning chamber is used to create a background plasma to study plasma wave resonance conditions [19].

4. Conclusion/Discussion

The results presented in this paper form the base for future plasma-cyclotron resonance experiments to be carried out. The initial AKR experiments prior to the addition of the Penning trap showed proof of mirroring with steadily decreasing beam current as the magnetic field was increased. For the dimensions of the waveguide the frequency was measured at 4.42GHz as expected close to cut off for the TE_{01} mode, with power of emitted radiation ~19-35kW. The efficiency of emission was calculated to be ~1-2%. These measurements compare well with magnetospheric observations but lack the presence of a background plasma.

The initial investigations demonstrating the ability of the Penning geometry to provide a background plasma lay a foundation to run experiments to analyze the instabilities of a beam which is passed through the plasma discharge in the Penning trap and to measure the radiation emitted. Detailed analysis with insertion of a plasma probe will allow plasma frequency, density and temperature to be determined which will enable comparisons to magnetospheric data.

References

[1] D.A. Gurnett, *Journal of Geophysical Research*, **79**, pp4227-4238 (1974)
[2] P.L. Pritchett & R.J. Strangeway, *Journal of Geophysical Research*, **90**, pp9650-9662 (1985)
[3] S.L. McConville et al, *Plasma Physics & Controlled Fusion* **50**, 074010 (2008)
[4] K. Ronald et al, *Plasma Sources Science & Technology* **17**, 035011 (2008)
[5] K. Ronald et al, *Physics of Plasmas* **15**, 056503 (2008)
[6] D.C. Speirs et al, *Plasma Physics & Controlled Fusion* **50**, 074011 (2008)
[7] K.M. Gillespie et al, *Plasma Physics & Controlled Fusion* **50**, 124038 (2008)
[8] D.C. Speirs et al, *Journal of Plasma Physics* **71**, pp665-674 (2005)
[9] D.C. Speirs et al, *Physics of Plasmas* **17**, 056501 (2010)
[10] R.Q. Twiss, *Australian Journal of Physics*, **11**, pp564-579 (1958)
[11] P. Sprangle & A.T. Drobot, *IEEE trans. on Microwave Theory and Techniques*, **MTT-25**(1977)
[12] R. Bingham & R.A. Cairns, *Physics of Plasmas*, **7**, pp3089-3092 (2000)
[13] R. Bingham & R.A. Cairns, *Physica Scripta*, **T98**, pp160-162 (2002)
[14] R. Bingham et al, *Contributions to Plasma Physics*, **44**, pp382-387 (2004)
[15] G.T. Delory et al, *Geophysical Research Letters*, **25**, pp2069-2072 (1998)
[16] R.E. Ergun et al, *The Astrophysical Journal*, **538**, pp456-466 (2000)
[17] R.A. Cairns et al, *Physica Scripta*, **T116**, pp23-26 (2005)
[18] I. Vorgul et al, *Physics of Plasmas*, **12**, pp1-8 (2005)
[19] J.E. Allen & A.D.R. Phelps, *Rep. Prog. Phys.*, **40**, pp1305-1368 (1977)